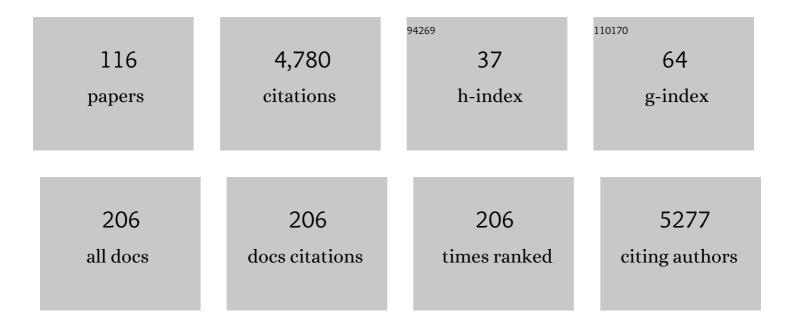
Andrey Kovalevsky

List of Publications by Year in descending order

Source: https://exaly.com/author-pdf/9316831/publications.pdf Version: 2024-02-01



#	Article	IF	CITATIONS
1	Photoinduced Linkage Isomers of Transition-Metal Nitrosyl Compounds and Related Complexes. Chemical Reviews, 2002, 102, 861-884.	23.0	411
2	Structural plasticity of SARS-CoV-2 3CL Mpro active site cavity revealed by room temperature X-ray crystallography. Nature Communications, 2020, 11, 3202.	5.8	334
3	Physical and Kinetic Analysis of the Cooperative Role of Metal Ions in Catalysis of Phosphodiester Cleavage by a Dinuclear Zn(II) Complex. Journal of the American Chemical Society, 2003, 125, 1988-1993.	6.6	224
4	Creating nanocavities of tunable sizes: Hollow helices. Proceedings of the National Academy of Sciences of the United States of America, 2002, 99, 11583-11588.	3.3	149
5	Metal Ion Roles and the Movement of Hydrogen during Reaction Catalyzed by D-Xylose Isomerase: A Joint X-Ray and Neutron Diffraction Study. Structure, 2010, 18, 688-699.	1.6	139
6	Ultra-high Resolution Crystal Structure of HIV-1 Protease Mutant Reveals Two Binding Sites for Clinical Inhibitor TMC114. Journal of Molecular Biology, 2006, 363, 161-173.	2.0	136
7	Supercomputer-Based Ensemble Docking Drug Discovery Pipeline with Application to Covid-19. Journal of Chemical Information and Modeling, 2020, 60, 5832-5852.	2.5	134
8	Amprenavir complexes with HIVâ€1 protease and its drugâ€resistant mutants altering hydrophobic clusters. FEBS Journal, 2010, 277, 3699-3714.	2.2	116
9	Malleability of the SARS-CoV-2 3CL Mpro Active-Site Cavity Facilitates Binding of Clinical Antivirals. Structure, 2020, 28, 1313-1320.e3.	1.6	108
10	The Catalytic Mechanism of an Aspartic Proteinase Explored with Neutron and X-ray Diffraction. Journal of the American Chemical Society, 2008, 130, 7235-7237.	6.6	106
11	Neutron Diffraction of Acetazolamide-Bound Human Carbonic Anhydrase II Reveals Atomic Details of Drug Binding. Journal of the American Chemical Society, 2012, 134, 14726-14729.	6.6	100
12	Unusual zwitterionic catalytic site of SARS–CoV-2 main protease revealed by neutron crystallography. Journal of Biological Chemistry, 2020, 295, 17365-17373.	1.6	97
13	Atomic resolution crystal structures of HIV-1 protease and mutants V82A and I84V with saquinavir. Proteins: Structure, Function and Bioinformatics, 2007, 67, 232-242.	1.5	84
14	Neutron Structure of Human Carbonic Anhydrase II: Implications for Proton Transfer. Biochemistry, 2010, 49, 415-421.	1.2	82
15	A new crystal form of human acetylcholinesterase for exploratory room-temperature crystallography studies. Chemico-Biological Interactions, 2019, 309, 108698.	1.7	82
16	Effect of Flap Mutations on Structure of HIV-1 Protease and Inhibition by Saquinavir and Darunavir. Journal of Molecular Biology, 2008, 381, 102-115.	2.0	81
17	First Observation of Photoinduced Nitrosyl Linkage Isomers of Iron Nitrosyl Porphyrins. Journal of the American Chemical Society, 2000, 122, 7142-7143.	6.6	75
18	The IMAGINE instrument: first neutron protein structure and new capabilities for neutron macromolecular crystallography. Acta Crystallographica Section D: Biological Crystallography, 2013, 69, 2157-2160.	2.5	73

#	Article	IF	CITATIONS
19	Toward resolving the catalytic mechanism of dihydrofolate reductase using neutron and ultrahigh-resolution X-ray crystallography. Proceedings of the National Academy of Sciences of the United States of America, 2014, 111, 18225-18230.	3.3	72
20	Covalent narlaprevir- and boceprevir-derived hybrid inhibitors of SARS-CoV-2 main protease. Nature Communications, 2022, 13, 2268.	5.8	69
21	Identification of the Elusive Hydronium Ion Exchanging Roles with a Proton in an Enzyme at Lower pHâ€Values. Angewandte Chemie - International Edition, 2011, 50, 7520-7523.	7.2	62
22	Joint X-ray/Neutron Crystallographic Study of HIV-1 Protease with Clinical Inhibitor Amprenavir: Insights for Drug Design. Journal of Medicinal Chemistry, 2013, 56, 5631-5635.	2.9	61
23	Direct visualization of critical hydrogen atoms in a pyridoxal 5′-phosphate enzyme. Nature Communications, 2017, 8, 955.	5.8	55
24	High-Throughput Virtual Screening and Validation of a SARS-CoV-2 Main Protease Noncovalent Inhibitor. Journal of Chemical Information and Modeling, 2022, 62, 116-128.	2.5	54
25	Neutron and Atomic Resolution X-ray Structures of a Lytic Polysaccharide Monooxygenase Reveal Copper-Mediated Dioxygen Binding and Evidence for N-Terminal Deprotonation. Biochemistry, 2017, 56, 2529-2532.	1.2	53
26	Neutron Structure of Human Carbonic Anhydrase II: A Hydrogen-Bonded Water Network "Switch―Is Observed between pH 7.8 and 10.0. Biochemistry, 2011, 50, 9421-9423.	1.2	52
27	Direct observation of hydrogen atom dynamics and interactions by ultrahigh resolution neutron protein crystallography. Proceedings of the National Academy of Sciences of the United States of America, 2012, 109, 15301-15306.	3.3	51
28	Room-temperature X-ray crystallography reveals the oxidation and reactivity of cysteine residues in SARS-CoV-2 3CL M ^{pro} : insights into enzyme mechanism and drug design. IUCrJ, 2020, 7, 1028-1035.	1.0	49
29	Mechanism of Drug Resistance Revealed by the Crystal Structure of the Unliganded HIV-1 Protease with F53L Mutation. Journal of Molecular Biology, 2006, 358, 1191-1199.	2.0	48
30	Neutron scattering in the biological sciences: progress and prospects. Acta Crystallographica Section D: Structural Biology, 2018, 74, 1129-1168.	1.1	47
31	Inhibitor binding influences the protonation states of histidines in SARS-CoV-2 main protease. Chemical Science, 2021, 12, 1513-1527.	3.7	47
32	Synthesis, Crystal Structures, Magnetic Properties and Photoconductivity of C60 and C70 Complexes with Metal Dialkyldithiocarbamates M(R2dtc)x, where M = Cull, Cul, Agl, Znll, Cdll, Hgll, Mnll, Nill, and Ptll; R = Me, Et, andnPr. European Journal of Inorganic Chemistry, 2006, 2006, 1881-1895.	1.0	44
33	Caught in the Act:  The 1.5 à Resolution Crystal Structures of the HIV-1 Protease and the I54V Mutant Reveal a Tetrahedral Reaction Intermediate. Biochemistry, 2007, 46, 14854-14864.	1.2	44
34	Structural Evidence for Effectiveness of Darunavir and Two Related Antiviral Inhibitors against HIV-2 Protease. Journal of Molecular Biology, 2008, 384, 178-192.	2.0	44
35	Hydrogen Location in Stages of an Enzyme-Catalyzed Reaction: Time-of-Flight Neutron Structure of d-Xylose Isomerase with Bound d-Xylulose. Biochemistry, 2008, 47, 7595-7597.	1.2	42
36	Longâ€Range Electrostaticsâ€Induced Twoâ€Proton Transfer Captured by Neutron Crystallography in an Enzyme Catalytic Site. Angewandte Chemie - International Edition, 2016, 55, 4924-4927.	7.2	42

#	Article	IF	CITATIONS
37	Design, Synthesis, Proteinâ ligand X-ray Structure, and Biological Evaluation of a Series of Novel Macrocyclic Human Immunodeficiency Virus-1 Protease Inhibitors to Combat Drug Resistance. Journal of Medicinal Chemistry, 2009, 52, 7689-7705.	2.9	40
38	"To Be or Not to Be" Protonated: Atomic Details of Human Carbonic Anhydrase-Clinical Drug Complexes by Neutron Crystallography and Simulation. Structure, 2018, 26, 383-390.e3.	1.6	40
39	Direct evidence that an extended hydrogen-bonding network influences activation of pyridoxal 5′-phosphate in aspartate aminotransferase. Journal of Biological Chemistry, 2017, 292, 5970-5980.	1.6	38
40	Structural aspects of two-stage dimerization in an ionic C60complex with bis(benzene)chromium: Cr(C6H6)2·C60·C6H4Cl2. Dalton Transactions, 2006, , 3716-3720.	1.6	36
41	Joint neutron crystallographic and NMR solution studies of Tyr residue ionization and hydrogen bonding: Implications for enzyme-mediated proton transfer. Proceedings of the National Academy of Sciences of the United States of America, 2015, 112, 5673-5678.	3.3	36
42	Direct Observation of Protonation State Modulation in SARS-CoV-2 Main Protease upon Inhibitor Binding with Neutron Crystallography. Journal of Medicinal Chemistry, 2021, 64, 4991-5000.	2.9	36
43	Direct Determination of Protonation States of Histidine Residues in a 2ÂÃ Neutron Structure of Deoxy-Human Normal Adult Hemoglobin and Implications for the Bohr Effect. Journal of Molecular Biology, 2010, 398, 276-291.	2.0	35
44	Direct determination of protonation states and visualization of hydrogen bonding in a glycoside hydrolase with neutron crystallography. Proceedings of the National Academy of Sciences of the United States of America, 2015, 112, 12384-12389.	3.3	35
45	X-ray crystallographic studies of family 11 xylanase Michaelis and product complexes: implications for the catalytic mechanism. Acta Crystallographica Section D: Biological Crystallography, 2014, 70, 11-23.	2.5	34
46	Structural, Electronic, and Electrostatic Determinants for Inhibitor Binding to Subsites S1 and S2 in SARS-CoV-2 Main Protease. Journal of Medicinal Chemistry, 2021, 64, 17366-17383.	2.9	32
47	Neutron Diffraction Reveals Hydrogen Bonds Critical for cGMP-Selective Activation: Insights for cGMP-Dependent Protein Kinase Agonist Design. Biochemistry, 2014, 53, 6725-6727.	1.2	31
48	Neutron structures of the <i>Helicobacter pylori</i> 5′-methylthioadenosine nucleosidase highlight proton sharing and protonation states. Proceedings of the National Academy of Sciences of the United States of America, 2016, 113, 13756-13761.	3.3	31
49	Solution Kinetics Measurements Suggest HIV-1 Protease Has Two Binding Sites for Darunavir and Amprenavir. Journal of Medicinal Chemistry, 2008, 51, 6599-6603.	2.9	30
50	High-resolution neutron crystallographic studies of the hydration of the coenzyme cob(II)alamin. Acta Crystallographica Section D: Biological Crystallography, 2011, 67, 584-591.	2.5	30
51	Neutron structure of human carbonic anhydrase II in complex with methazolamide: mapping the solvent and hydrogen-bonding patterns of an effective clinical drug. IUCrJ, 2016, 3, 319-325.	1.0	27
52	Low- and room-temperature X-ray structures of protein kinase A ternary complexes shed new light on its activity. Acta Crystallographica Section D: Biological Crystallography, 2012, 68, 854-860.	2.5	26
53	The Neutron Macromolecular Crystallography Instruments at Oak Ridge National Laboratory: Advances, Challenges, and Opportunities. Crystals, 2018, 8, 388.	1.0	26
54	Zooming in on protons: Neutron structure of protein kinase A trapped in a product complex. Science Advances, 2019, 5, eaav0482.	4.7	26

#	Article	IF	CITATIONS
55	Room Temperature Neutron Crystallography of Drug Resistant HIV-1 Protease Uncovers Limitations of X-ray Structural Analysis at 100 K. Journal of Medicinal Chemistry, 2017, 60, 2018-2025.	2.9	25
56	Mannobiose Binding Induces Changes in Hydrogen Bonding and Protonation States of Acidic Residues in Concanavalin A As Revealed by Neutron Crystallography. Biochemistry, 2017, 56, 4747-4750.	1.2	25
57	IMAGINE: neutrons reveal enzyme chemistry. Acta Crystallographica Section D: Structural Biology, 2018, 74, 778-786.	1.1	25
58	Michaelis-like complex of SARS-CoV-2 main protease visualized by room-temperature X-ray crystallography. IUCrJ, 2021, 8, 973-979.	1.0	25
59	Insights into the Phosphoryl Transfer Catalyzed by cAMP-Dependent Protein Kinase: An X-ray Crystallographic Study of Complexes with Various Metals and Peptide Substrate SP20. Biochemistry, 2013, 52, 3721-3727.	1.2	24
60	Rational design, synthesis, and evaluation of uncharged, "smart―bis-oxime antidotes of organophosphate-inhibited human acetylcholinesterase. Journal of Biological Chemistry, 2020, 295, 4079-4092.	1.6	24
61	The mechanisms of catalysis and ligand binding for the SARS-CoV-2 NSP3 macrodomain from neutron and x-ray diffraction at room temperature. Science Advances, 2022, 8, .	4.7	24
62	L-Arabinose Binding, Isomerization, and Epimerization by D-Xylose Isomerase: X-Ray/Neutron Crystallographic and Molecular Simulation Study. Structure, 2014, 22, 1287-1300.	1.6	22
63	Phosphoryl Transfer Reaction Snapshots in Crystals. Journal of Biological Chemistry, 2015, 290, 15538-15548.	1.6	22
64	Protein Kinase A Catalytic Subunit Primed for Action: Time-Lapse Crystallography of Michaelis Complex Formation. Structure, 2015, 23, 2331-2340.	1.6	22
65	IMAGINE: The neutron protein crystallography beamline at the high flux isotope reactor. Methods in Enzymology, 2020, 634, 69-85.	0.4	21
66	Room-temperature neutron and X-ray data collection of 3CL M ^{pro} from SARS-CoV-2. Acta Crystallographica Section F, Structural Biology Communications, 2020, 76, 483-487.	0.4	21
67	Synthesis, crystal structure and photoconductivity of the first [60]fullerene complex with metal diethyldithiocarbamate: {Cull(dedtc)2}2·C60. Dalton Transactions, 2005, , 1821.	1.6	20
68	Evolution and characterization of a new reversibly photoswitching chromogenic protein, Dathail. Journal of Molecular Biology, 2016, 428, 1776-1789.	2.0	20
69	Inorganic pyrophosphatase crystals from <i>Thermococcus thioreducens</i> for X-ray and neutron diffraction. Acta Crystallographica Section F: Structural Biology Communications, 2012, 68, 1482-1487.	0.7	19
70	Engineering acidic Streptomyces rubiginosus D-xylose isomerase by rational enzyme design. Protein Engineering, Design and Selection, 2014, 27, 59-64.	1.0	19
71	Inhibition of <scp>D</scp> -xylose isomerase by polyols: atomic details by joint X-ray/neutron crystallography. Acta Crystallographica Section D: Biological Crystallography, 2012, 68, 1201-1206.	2.5	18
72	Metal-Free cAMP-Dependent Protein Kinase Can Catalyze Phosphoryl Transfer. Biochemistry, 2014, 53, 3179-3186.	1.2	18

#	Article	IF	CITATIONS
73	Potent HIV-1 protease inhibitors incorporating meso-bicyclic urethanes as P2-ligands: structure-based design, synthesis, biological evaluation and protein–ligand X-ray studies. Organic and Biomolecular Chemistry, 2008, 6, 3703.	1.5	17
74	Novel complex MAD phasing and RNase H structural insights using selenium oligonucleotides. Acta Crystallographica Section D: Biological Crystallography, 2014, 70, 354-361.	2.5	17
75	Limitations in current acetylcholinesterase structure–based design of oxime antidotes for organophosphate poisoning. Annals of the New York Academy of Sciences, 2016, 1378, 41-49.	1.8	17
76	Hit Expansion of a Noncovalent SARS-CoV-2 Main Protease Inhibitor. ACS Pharmacology and Translational Science, 2022, 5, 255-265.	2.5	17
77	Understanding the pH-Dependent Reaction Mechanism of a Glycoside Hydrolase Using High-Resolution X-ray and Neutron Crystallography. ACS Catalysis, 2018, 8, 8058-8069.	5.5	15
78	Hyperconjugation Promotes Catalysis in a Pyridoxal 5â€2-Phosphate-Dependent Enzyme. ACS Catalysis, 2018, 8, 6733-6737.	5.5	15
79	Capturing the Reaction Pathway in Near-Atomic-Resolution Crystal Structures of HIV-1 Protease. Biochemistry, 2012, 51, 7726-7732.	1.2	13
80	Productive reorientation of a bound oxime reactivator revealed in room temperature X-ray structures of native and VX-inhibited human acetylcholinesterase. Journal of Biological Chemistry, 2019, 294, 10607-10618.	1.6	13
81	Macromolecular neutron crystallography at the Protein Crystallography Station (PCS). Acta Crystallographica Section D: Biological Crystallography, 2010, 66, 1206-1212.	2.5	11
82	Biological Structures. Experimental Methods in the Physical Sciences, 2017, 49, 1-75.	0.1	10
83	Pyridoxal 5′-phosphate dependent reactions: Analyzing the mechanism of aspartate aminotransferase. Methods in Enzymology, 2020, 634, 333-359.	0.4	10
84	Room-temperature ultrahigh-resolution time-of-flight neutron and X-ray diffraction studies of H/D-exchanged crambin. Acta Crystallographica Section F: Structural Biology Communications, 2012, 68, 119-123.	0.7	9
85	Neutron and high-resolution room-temperature X-ray data collection from crystallized lytic polysaccharide monooxygenase. Acta Crystallographica Section F, Structural Biology Communications, 2015, 71, 1448-1452.	0.4	8
86	Capturing the Catalytic Proton of Dihydrofolate Reductase: Implications for General Acid–Base Catalysis. ACS Catalysis, 2021, 11, 5873-5884.	5.5	8
87	Characterization and structural analysis of a thermophilic GH11 xylanase from compost metatranscriptome. Applied Microbiology and Biotechnology, 2021, 105, 7757-7767.	1.7	8
88	Covalent inhibition of hAChE by organophosphates causes homodimer dissociation through long-range allosteric effects. Journal of Biological Chemistry, 2021, 297, 101007.	1.6	8
89	Anion Chain Structure Controlled Behavior of Phase Transition in Quasi-Two-Dimensional Organic Metal (EDT-TTF)4[Hg3l8]1â^'x. Crystal Growth and Design, 2007, 7, 2768-2773.	1.4	7
90	Preliminary joint X-ray and neutron protein crystallographic studies of ecDHFR complexed with folate and NADP ⁺ . Acta Crystallographica Section F, Structural Biology Communications, 2014, 70, 814-818.	0.4	7

ANDREY KOVALEVSKY

#	Article	IF	CITATIONS
91	Visualizing the Bohr effect in hemoglobin: neutron structure of equine cyanomethemoglobin in the R state and comparison with human deoxyhemoglobin in the T state. Acta Crystallographica Section D: Structural Biology, 2016, 72, 892-903.	1.1	7
92	Substrate Binding Stiffens Aspartate Aminotransferase by Altering the Enzyme Picosecond Vibrational Dynamics. ACS Omega, 2020, 5, 18787-18797.	1.6	7
93	Protonation states of histidine and other key residues in deoxy normal human adult hemoglobin by neutron protein crystallography. Acta Crystallographica Section D: Biological Crystallography, 2010, 66, 1144-1152.	2.5	6
94	Preliminary joint X-ray and neutron protein crystallographic studies of endoxylanase II from the fungus <i>Trichoderma longibrachiatum</i> . Acta Crystallographica Section F: Structural Biology Communications, 2011, 67, 283-286.	0.7	6
95	Longâ€Range Electrostaticsâ€Induced Twoâ€Proton Transfer Captured by Neutron Crystallography in an Enzyme Catalytic Site. Angewandte Chemie, 2016, 128, 5008-5011.	1.6	6
96	Pressure and Temperature Effects on the Formation of Aminoacrylate Intermediates of Tyrosine Phenol-lyase Demonstrate Reaction Dynamics. ACS Catalysis, 2020, 10, 1692-1703.	5.5	6
97	Visualizing Tetrahedral Oxyanion Bound in HIV-1 Protease Using Neutrons: Implications for the Catalytic Mechanism and Drug Design. ACS Omega, 2020, 5, 11605-11617.	1.6	6
98	Room temperature crystallography of human acetylcholinesterase bound to a substrate analogue 4K-TMA: Towards a neutron structure. Current Research in Structural Biology, 2021, 3, 206-215.	1.1	6
99	Using neutron protein crystallography to understand enzyme mechanisms. Acta Crystallographica Section D: Biological Crystallography, 2010, 66, 1257-1261.	2.5	5
100	Microgravity crystallization of perdeuterated tryptophan synthase for neutron diffraction. Npj Microgravity, 2022, 8, 13.	1.9	5
101	Preliminary joint neutron time-of-flight and X-ray crystallographic study of human ABO(H) blood group A glycosyltransferase. Acta Crystallographica Section F: Structural Biology Communications, 2011, 67, 258-262.	0.7	4
102	Temperature-Induced Replacement of Phosphate Proton with Metal Ion Captured in Neutron Structures of A-DNA. Structure, 2018, 26, 1645-1650.e3.	1.6	4
103	Proton transfer and drug binding details revealed in neutron diffraction studies of wild-type and drug resistant HIV-1 protease. Methods in Enzymology, 2020, 634, 257-279.	0.4	4
104	EWALD: A macromolecular diffractometer for the second target station. Review of Scientific Instruments, 2022, 93, .	0.6	4
105	Joint neutron/molecular dynamics vibrational spectroscopy reveals softening of HIV-1 protease upon binding of a tight inhibitor. Physical Chemistry Chemical Physics, 2022, 24, 3586-3597.	1.3	3
106	Heterologous expression, purification, crystallization and preliminary X-ray analysis ofTrichoderma reeseixylanase II and four variants. Acta Crystallographica Section F: Structural Biology Communications, 2013, 69, 320-323.	0.7	2
107	Studying the Role of a Single Mutation of a Family 11 Glycoside Hydrolase Using High-Resolution X-ray Crystallography. Protein Journal, 2020, 39, 671-680.	0.7	2
108	Room-temperature photo-induced martensitic transformation in a protein crystal. IUCrJ, 2019, 6, 619-629.	1.0	2

#	Article	IF	CITATIONS
109	Hemoglobin redux: combining neutron and X-ray diffraction with mass spectrometry to analyse the quaternary state of oxidized hemoglobins. Acta Crystallographica Section D: Biological Crystallography, 2010, 66, 1249-1256.	2.5	1
110	Time-of-flight neutron diffraction study of bovine γ-chymotrypsin at the Protein Crystallography Station. Acta Crystallographica Section F: Structural Biology Communications, 2011, 67, 587-590.	0.7	1
111	Neutron Crystallography Detects Differences in Protein Dynamics: Structure of the PKG II Cyclic Nucleotide Binding Domain in Complex with an Activator. Biochemistry, 2018, 57, 1833-1837.	1.2	1
112	Revertant mutation V48G alters conformational dynamics of highly drug resistant HIV protease PRS17. Journal of Molecular Graphics and Modelling, 2021, 108, 108005.	1.3	1
113	Direct observation of protonation states in a PLP-dependent enzyme by neutron crystallography. Acta Crystallographica Section A: Foundations and Advances, 2017, 73, a26-a26.	0.0	1
114	Bis[bis(3-phenylpyrazol-1-yl)(pyrazol-1-yl)methane]copper(II) bis(perchlorate) acetonitrile disolvate. Acta Crystallographica Section C: Crystal Structure Communications, 2006, 62, m30-m32.	0.4	0
115	Neutron protein crystallography reveals unique details of clinical drug binding to a human target enzyme. Neutron News, 2013, 24, 20-23.	0.1	0
116	Protein kinase A in the neutron beam: Insights for catalysis from directly observing protons. Methods in Enzymology, 2020, 634, 311-331.	0.4	0